Screening of *SPATA7* in Patients with Leber Congenital Amaurosis and Severe Childhood-Onset Retinal Dystrophy Reveals Disease-Causing Mutations

Donna S. Mackay,[1] *Louise A. Ocaka,*[1] *Arundhati Dev Borman,*[1,2] *Panagiotis I. Sergouniotis,*[1,2] *Robert H. Henderson,*[2] *Phillip Moradi,*[2] *Anthony G. Robson,*[1,2] *Dorothy A. Thompson,*[3,4] *Andrew R. Webster,*[1,2] *and Anthony T. Moore*[1,2]

Purpose. To investigate the prevalence of sequence variants in the gene *SPATA7* in patients with Leber congenital amaurosis (LCA) and autosomal recessive, severe, early-onset retinal dystrophy (EORD) and to delineate the ocular phenotype associated with *SPATA7* mutations.

Methods. Patients underwent standard ophthalmic evaluation after providing informed consent. One hundred forty-one DNA samples from patients with LCA and EORD had been analyzed for mutations by using a microarray, with negative results. One additional patient underwent *SPATA7* screening due to a region of autozygosity surrounding this gene. A further patient was screened who had a compatible ocular phenotype. The entire *SPATA7* coding sequence was assayed, including the intron–exon junctions, by using a combination of direct DNA sequencing and high-resolution melting screening.

Results. Screening of *SPATA7* identified several known and novel single-nucleotide polymorphisms (SNPs). Affected individuals from five unrelated families were identified to have coding changes. Clinical features demonstrated a severe infantile onset retinal dystrophy, similar to Leber congenital amaurosis. The retina had widespread retinal pigment epithelial atrophy, with minimal pigment migration into the neurosensory retina. Fundus autofluorescence imaging showed a parafoveal annulus of increased autofluorescence. High-definition optical coherence tomography showed preservation of the inner segment/outer segment junction at the fovea.

Conclusions. Mutations in *SPATA7* are a rare cause of childhood retinal dystrophy accounting for 1.7% of disease in this cohort. Affected patients present in infancy with severe visual loss, but may have some preservation of the photoreceptor structure in the central retina. (*Invest Ophthalmol Vis Sci.* 2011;52:3032–3038) DOI:10.1167/iovs.10-7025

Leber congenital amaurosis (LCA), first described by Theodor Leber in 1869,[1] is a generalized retinal dystrophy which presents at birth, or soon after, with severe visual impairment and nystagmus. LCA accounts for 3% to 5% of childhood blindness in the developed world and has an incidence of 2 to 3 per 100,000 live births.[2] The clinical features include severe visual loss, sluggish pupillary responses, and roving eye movements. The retinal appearance may be normal at diagnosis, or there may be a variety of abnormalities, including macular atrophy, peripheral white dots at the level of the retinal pigment epithelium (RPE), RPE atrophy, and/or retinal pigmentation. The full-field electroretinogram (ERG) is usually unrecordable.[3,4]

Most forms of LCA are inherited as an autosomal recessive (AR) trait, although rare dominant forms have been reported. To date, 14 causative genes (*GUCY2D*,[5] *AIPL1*,[6] *RPE65*,[7] *RPGRIP1*,[8] *CRX*,[9] *TULP1*,[10] *CRB1*,[11] *RDH12*,[12] *CEP290*,[13] *LCA5*,[14] *SPATA7*,[15] *LRAT*,[16] *MERTK*[17] and *IQCB1*[18]) with one further locus, LCA9,[19] have been reported to be associated with autosomal recessive LCA. Mutations in some of these genes are also associated with severe rod–cone dystrophies presenting later in childhood.

The LCA3 locus was identified in 1998[20] by linkage analysis in a large consanguineous family from Saudi Arabia. A second family, also from Saudi Arabia, was found to map to the same region of chromosome 14. *RDH12*, a positional candidate, was excluded as the disease gene, suggesting that this locus represented a novel gene for LCA.[21] In 2009, *SPATA7* was identified as the causative gene at this locus after further fine mapping of one of the linked families.[15] Four novel mutations were found in five families with LCA or juvenile onset retinitis pigmentosa (RP). Recently, a further four families with six mutations (four of which were novel) have been identified.[22]

SPATA7 (spermatogenesis associated protein 7) was first cloned in 2003 from the rat testis and called RSD-3/HSD-3.1.[23] The corresponding human cDNA was also found to be expressed in the human testis. The human gene (MIM 609868; Mendelian Inheritance in Man; National Center for Biotechnology Information, Bethesda, MD) consisted of 12 exons that spanned approximately 52.8 kb and mapped to chromosome 14, region q31.3. The gene encodes a protein of 599 amino acids. It is conserved from sea urchin to human, but is absent in lower eukaryotes.[15] Analysis of the protein using the PSIPred program (provided in the public domain by Bioinformatics Group, Department of Computer Science, University College London, at http://bioinf.cs.ucl.ac.uk/introduction) showed

From the [1]Department of Genetics, Institute of Ophthalmology, London, United Kingdom; [2]Moorfields Eye Hospital, London, United Kingdom; the [3]Clinical and Academic Department of Ophthalmology, Great Ormond Street Hospital for Children, London, United Kingdom; and the [4]Institute of Child Health, University College London, United Kingdom.

Supported by Fight for Sight Grant 1624 (UK), the National Institute for Health Research UK (Moorfields Eye Hospital Biomedical Research Centre, London, UK), Alexander S. Onassis Public Benefit Foundation (Greece), the Foundation Fighting Blindness (USA), and the Ulverscroft foundation.

Submitted for publication December 9, 2010; revised January 11, 2011; accepted January 11, 2011

Disclosure: **D.S. Mackay**, None; **L.A. Ocaka**, None; **A.D. Borman**, None; **P.I. Sergouniotis**, None; **R.H. Henderson**, None; **P. Moradi**, None; **A.G. Robson**, None; **D.A. Thompson**, None; **A.R. Webster**, None; **A.T. Moore**, None

Corresponding author: Donna S. Mackay, Department of Genetics, Institute of Ophthalmology, 11-43 Bath Street, London, UK EC1V 9EL; d.mackay@ucl.ac.uk.

one transmembrane domain but no known functional domains. Expression in the mouse retina was found in multiple retinal layers, including the ganglion cell and inner nuclear layers and in the inner segments of photoreceptors. Expression levels at different time points suggested that *Spata7* is important for normal retinal function rather than development.[15] A recent report on the *Spata7*-knockout mouse suggested that the protein is involved in protein transport (Abulimiti Sr A, et al. *IOVS* 2010;51:ARVO E-Abstract 723).

Two isoforms of SPATA7 are known to be expressed.[24] Expression analysis of these two isoforms in 22 adult and fetal human tissues showed high levels in the retina, cerebellum, whole brain, and testis. Isoform 1 was more highly expressed than was isoform 2 (missing exon 3) in neuronal tissues, whereas isoform 2 was highly expressed in the testis.[22]

To evaluate the role of *SPATA7* in childhood-onset retinal dystrophies in the British population, we screened 141 patients with LCA or early childhood onset severe retinal dystrophy for all the coding exons, using a combination of melting curve analysis and Sanger sequencing. We also investigated the phenotype associated with *SPATA7* mutations.

Materials and Methods

Clinical Investigations

All patients in this study had a clinical diagnosis of LCA or severe AR retinal dystrophy with symptom onset before 6 years of age. All provided informed consent as part of a research project approved by the local research ethics committee, and all investigations were conducted in accordance with the principles of the Declaration of Helsinki. A clinical evaluation, including monocular best corrected visual acuity (BCVA), perimetry, and slit lamp biomicroscopy was performed on all patients who could cooperate with testing. Patients underwent retinal imaging (TRC 501A retinal camera; Topcon Corp., Tokyo, Japan) and, where possible, high-resolution spectral domain optical coherence tomography (SD-OCT; Spectralis Spectral domain OCT scanner; Heidelberg Engineering, Germany) and retinal autofluorescence (AF) imaging with a confocal scanning laser ophthalmoscope (Zeiss Prototype; Carl Zeiss Meditec, GmbH, Oberkochen, Germany). Pattern and full-field electroretinography (PERG and ERG) were performed in consideration of the recommendations of the International Society for Clinical Electrophysiology of Vision (ISCEV) or using a modified pediatric ERG protocol with skin electrodes, as previously described.[25–28]

Blood samples were collected in EDTA tubes, and DNA was extracted with a blood-extraction kit (Puregene; Invitrogen, Paisley, UK), according to the manufacturer's instructions.

From a total of 292 subjects recruited into this study, DNA samples from 141 subjects with no known mutations in LCA genes were chosen for *SPATA7* mutation screening.

Microarray SNP6 Autozygosity Mapping

Subject 2 from family 3 was chosen for analysis with a gene microarray (SNP6.0 array; Affymetrix, Santa Clara, CA), according to the manufacturer's instructions. Genotypes for single-nucleotide polymorphisms (SNPs) were called by gene analysis software (GeneChip DNA Analysis Software; GDAS ver. 3.0; Affymetrix). Regions of homozygosity were also identified on computer (AutoSNPa; provided in the public domain by the Leeds Institute of Molecular Medicine, University of Leeds, UK, at http://dna.leeds.ac.uk/autospna/).[29]

Mutation Screening

Primers used to amplify the coding exons and the intron-exon boundaries of *SPATA7* were designed by hand. Primer sequences are shown in Table 1. Exons 2 to 5 were initially screened with the high-resolution melting curve technique (LightScanner; Idaho Technology, Salt Lake City, UT), with abnormal melting curves identified and then sequenced. All other exons were directly sequenced. All standard polymerase chain reactions (PCRs) were performed in a total volume of 30 μL containing 200 μM dNTPs (VH Bio, Gateshead, UK), 20 μM of each primer, 1× reaction buffer including 1.5 mM $MgCl_2$ (VH Bio), with 1

Table 1. Primers and PCR Conditions for *SPATA7*

Exon	Primer	Temp. (°C)	PCR Annealing (°C)	$MgCl_2$ Conc. (mM)	Size of Fragment (bp)	Analysis
Exon 1F	CAACTGTCCTCCTAGTACC	53.4	51	1.5	313	Sequencing
Exon 1R	TTGCACTCAGCTGCCCGGAC	73.2				
Exon 2F	GCTGTAACTCAGACTTCCTG	56.6	65	1.5	270	Melting curve
Exon 2R	TTGCCAGTAAAGGAAACACTC	60.7				
Exon 3F	GCTTCACATCACAATGTCATA	58.6	65	1.5	320	Melting curve
Exon 3R	CCAAACAAATACAAATCCTCTC	59.0				
Exon 4F	GGATCTTGTGTTTTCCATCGCT	66.2	65	1.5	293	Melting curve
Exon 4R	GAGAGTTCTGGAGGTAGTAGTT	54.8				
Exon 5F	ATATCTAGAGGCACATGTGA	54.5	65	1.5	409	Melting curve
Exon 5R	TGTACCACTAAAGAAGTACC	50.7				
Exon 6.1F	GTAAACCCTTGAGGCTATCAT	58.6	56	2.0	354	Sequencing
Exon 6.1R	CACTGGGTGCTTTCGAAATGA	67.2				
Exon 6.2F	CAGTGTGGATTATGCAGCCT	62.7	62	1.5	356	Sequencing
Exon 6.2R	CTTAAGGCTGGCAGCAGAAA	64.4				
Exon 7F	TTTTCTAGCCAGTAAACCTTG	57.7	55	3.0	152	Sequencing
Exon 7R	GCTGTACATATTCTATTTACTG	50.1				
Exon 8F	CTGGATATCTCTGTTCAATC	53.5	50	1.5	291	Sequencing
Exon 8R	CCAAAATAGATTGGAGCATGC	63.2				
Exon 9F	GGGCTATTCAGTGTGTACTA	54.2	56	2.0	170	Sequencing
Exon 9R	GGTTTCTTTGATTCTTAATCC	58.6				
Exon 10F	GTACATTGGTAATGGTAGAG	50.9	58	2.0	358	Sequencing
Exon 10R	TCTCCCAAGTGGTGAACTTC	61.7				
Exon 11F	CCTTTGTAGTTTCAGTGTTACGTAGCTAG	64.0	50	2.0	269	Sequencing
Exon 11R	TTCCTTTCACTTCTCCCACCAC	66.3				
Exon 12.1F	CGACTGTTCGAGCGACATATAA	63.9	60	2.5	667	Sequencing
Exon 12.1R	TCAGGGTCACTATCACCTTCAATG	66.0				
Exon 12.2F	CACCAAAGGATGAGAACGAGA	64.1	56	1.5	413	Sequencing
Exon 12.2R	GCAGCACAGAAAACCAATAGAG	62.4				

TABLE 2. SNPs Identified in *SPATA7* in the Study Cohort, with Allele Frequencies Compared to the Caucasian HapMap Frequencies

rs Number	Position	Nucleotide Change	Amino Acid Change	Allele Freq (in cohort)	HapMap CEU Allele Freq
rs709886	5′UTR	c.1−132A>G	—	A=0.000 G=1.000	A=0.000 G=1.000
Novel	5′UTR	c.1−42A>G	—	A=0.003 G=0.996	N/D
rs4904448	Exon 1	c.4G>A	p.D2N	G=0.664 A=0.336	G=0.548 A=0.458
Novel	Intro 1	c.20−19T>G	—	T=0.915 G=0.085	N/D
Novel	Exon 2	c.23G>A	p.R8L	G=0.833 A=0.167	N/D
Novel	Exon 2	c.44G>A	p.R15L	G=0.789 A=0.211	N/D
rs17124616	Intron 2	c.94+20C>T	—	C=0.993 T=0.007	N/D
Novel	Intron 3	c.190+74A>G	—	A=0.996 G=0.004	N/D
Novel	Intron 3	c.190+80A>G	—	A=0.996 G=0.004	N/D
Novel	Intron 3	c.190−16T>C	—	T=0.996 C=0.004	N/D
rs3179969	Exon 4	c.220G>A	p.V74M	G=0.873 A=0.127	G=0.683 A=0.317
rs61747004	Exon 5	c.284A>G	p.Q94L	A=0.993 G=0.007	N/D
rs35137272	Exon 5	c.357T>G	p.F119L	T=0.989 G=0.011	T=1.00
rs17124662	Exon 6	c.494G>A	p.S165N	G=0.993 A=0.007	G=1.00
Novel	Exon 6	c.729C>T	p.R242R	C=0.996 T=0.004	N/D
rs10139784	Exon 12	c.1602G>A	p.R534Q	G=0.996 A=0.004	G=1.00
Novel	Exon 12	c.1603G>T	p.R534R	G=0.996 T=0.004	N/D

unit of polymerase (Moltaq; VHBio) and 100 ng of DNA. PCR was performed on a thermal cycler (PTC200 DNA; Bio-Rad, Hemel Hempstead, UK). Cycling conditions were as follows: 2 minutes of denaturation at 95°C followed by 35 cycles of 94°C for 30 seconds, annealing temperature for 30 seconds, and extension at 72°C for 45 seconds. A final extension of 72°C for 7 minutes completed the cycling conditions. The annealing temperatures for each PCR are shown in Table 1.

PCR products were visualized on a 2% agarose gel containing 0.05% ethidium bromide. The products were cleaned using multiscreen PCR filter plates (catalog no. LSKMPCR10, Millipore, Watford, UK) before sequencing. PCR products were sequenced directly with dye-termination chemistry (Prism Big Dye terminator Kit ver. 3.1; ABI) in a 10-μL reaction. Samples were purified with a cleanup kit (Montage, catalog no. LSK509624; Millipore) before being run on a DNA sequencer (3730 DNA sequencer; ABI).

Electropherograms were analyzed for sequence changes using computational software (DNAStar, Inc., Madison, WI). Sequencing data obtained from PCR products were analyzed with, a program (SeqMan; DNAStar) designed to detect potential alterations in the sequence;. Any sequence changes identified were checked visually.

High-Resolution Melting Curve Analysis

Primers for exons 2 to 5 were designed using primer design software (LightScanner; Idaho Technology). Optimal PCR annealing temperatures were evaluated by using a gradient PCR setup of 55°C to 70°C. PCR was performed in a total volume of 10 μL containing 20 ng of genomic DNA, 4 μL of mastermix containing dye (LCGreen Plus; Idaho Technology), 2.5 μM of each primer, and molecular grade water. Mineral oil (15 μL per reaction), necessary for the system melting step, was added before cycling. PCR was performed on a DNA engine thermal cycler (model PTC200; Bio-Rad, Hemel Hempstead, UK). Cycling conditions were as follows: 2 minutes of denaturation at 95°C followed by 45 cycles of 94°C for 30 seconds and annealing temperature for 30 seconds. Heteroduplexes were generated by adding a step at 94°C for 30 seconds followed by cooling of the reactions to 28°C.

The melting run conditions were set according to the manufacturer's instructions. The start temperature was routinely set at 75°C with the end temperature at 94°C. The hold temperature was set at 72°C. Samples were analyzed by using the system software (ver. 2.0; Idaho Technology, Salt Lake City, UT). Samples that demonstrated abnormal melting curve patterns in comparison to standard melting curves were investigated further and sequenced.

RESULTS

Screening of *SPATA7* in LCA and EORD Patients

Screening of 141 probands with LCA/EORD revealed 21 sequence variants, when compared with the human genome sequence obtained from Ensembl (http://www.ensembl.org/index.html[30]) (Tables 2, 3). Table 2 shows the SNPs in *SPATA7* that were identified in this study. Seventeen SNPs were identified, of which nine are novel. The frequency of prevalence was calculated and, when possible, compared to the European Caucasian frequency from HapMap (http://hapmap.ncbi.nlm.nih.gov/, provided by the NCBI, Bethesda, MD). In most cases, the frequencies were similar. Ten of these SNPs caused coding changes (Tables 2, 3).

Four of the sequence variants were considered to be disease causing (Table 3). Three of four variants were predicted to

TABLE 3. Mutations Identified in *SPATA7*

Family	Consanguineous	Subject	Allele 1	Exon	Allele 2	Exon	Reference
1	Yes	1	c.253C>T, p.R85X	5	c.253C>T, p.R85X	5	Novel to this study
2	Yes	2	c.253C>T, p.R85X	5	c.253C>T, p.R85X	5	Novel to this study
3	Yes	3	c.253C>T, p.R85X	5	c.253C>T, p.R85X	5	Novel to this study
4	Yes	4	c.961dupA, p.P321TfsX5	8	c.961dupA, p.P321TfsX325	8	Wang et al.[15]
		5					
		6					
		7					
		8					
5	No	9	c.265_268delCTCA, p.L89KfsX3	5	c.1227_1229delCAC, p.H410del	12	Novel to this study
		10					

cause a premature termination of the SPATA7 protein. Five probands were identified as having disease caused by mutations in *SPATA7.*

Family 1 was a consanguineous family of Pakistani origin. One affected individual from this family (subject 1) was homozygous for a cytosine-to-thymine transition at nucleotide 253 in exon 5 of *SPATA7*. This mutation is predicted to cause the replacement of arginine at position 85 by a stop codon (p.R85X). No other family members were available for analysis.

Family 2 was chosen for screening based on a similar phenotype to other SPATA7 families. Subject 2 (family 2) is the product of a consanguineous marriage of Pakistani origin. There is no evidence to suggest that families 1 and 2 are related. Subject 2 was homozygous for the same cytosine-to-thymine transition at nucleotide 253, causing a p.R85X mutation. DNA analysis from this individual's mother for the p.R85X mutation confirmed its presence in the heterozygous state, thereby confirming segregation within this family. Paternal DNA was not available for analysis.

Family 3 was a consanguineous family of Bangladeshi origin. This family had undergone autozygosity mapping. The SNP microarray data (SNP6.0; Affymetrix) on subject 3 showed 11 regions of homozygosity over 10 Mb in size. The smallest region at 11 Mb contained *SPATA7*. Sequence analysis of subject 3 identified the same p.R85X mutation as families 1 and 2. Segregation analysis confirmed that both parents were carriers of the mutation. An affected brother was unavailable for molecular analysis.

Family 4 was a large consanguineous family of Pakistani origin. Sequencing of exon 8 in the proband (subject 4) identified a duplication of an adenine in both strands. This mutation (c.961dupA, p.P321TfsX5) has been published.[15] Sequence analysis of exon 8 in the family showed that the mutation segregated with disease and that all affected members of the family (subjects 4–8) were homozygous for this change.

Family 5, a nonconsanguineous family of British Caucasian origin, consisted of two affected brothers. Sequence analysis of these individuals (subjects 9 and 10) showed two novel changes in exons 5 and 12. In exon 5, a deletion of 4 bases (c.265_268delCTCA) was identified in the heterozygous state. This deletion is predicted to cause a frameshift (p.L89KfsX3). In exon 12, a further heterozygous deletion was found, consisting of 3 bases (c1227_1229delCAC) deleting a histidine at amino acid 410 (p.H410del). The brothers were identified to have inherited the exon 5 deletion from their mother and the exon 12 deletion from their father.

Clinical Features

Patient demographics, presenting features, general health, and ocular examination are summarized in Table 4. Eight of 10 patients were male. Patients 1 to 9 had clinical features consistent with LCA, having severe visual loss from early infancy, pendular nystagmus, and sluggish pupillary responses. Patient 10 had a milder phenotype with onset of nystagmus at 8 weeks of age. He was able to fix and follow at this age. When older, he was noted to have severe nyctalopia and constricted visual fields. These symptoms deteriorated significantly from 14 years of age. The clinical features in all the other patients remained unchanged over time. General health was good for most of the patients, except for patient 1 who had type II diabetes mellitus, auditory dysfunction requiring hearing aids, and fertility dysfunction (reduced spermatozoa count). In family 4, patient 6 had mild renal dysfunction, and patient 7 had severe autistic spectrum disorder and bilateral moderate to severe hearing loss. No other patients in this cohort had fertility or auditory dysfunction.

Visual acuity was hand movements or worse in patients 1 and 3 to 9. Patient 2 had an unaided VA of 1.08 logMAR in the

Table 4. Table of Clinical Features for *SPATA7* Patients in This Study

Family	Subject (Sex)	Ethnicity	Age at Onset	Age at Exam (y)	Symptoms				General Health	Presenting VA (logMAR)		Slit Lamp Examination
					Nystagmus	Nyctalopia	Photoattraction/ Aversion	VF		Right	Left	
1	1 (M)	Pakistani	Birth	43	√	?	X	NR	Type II diabetes mellitus Hearing ↓ Fertility ↓	HM	PL	Keratoconus PCIOL PSCLO
2	2 (F)	Pakistani	Birth	17	√	?	X	ND	Good	1.08	1.48	NAD
3	3 (M)	Bangladeshi	8 wk	15	√	X	Aversion	ND	Good	CF	CF	NAD
4	4 (M)	Pakistani	Birth	27	√	X	Aversion	NR	Good	HM	HM	NAD
	5 (M)	Pakistani	Birth	29	√	√	Aversion	NR	Good	HM	HM	NAD
	6 (M)	Pakistani	Birth	5	√	X	X	NR	Mild renal dysfunction	LP	LP	NAD
	7 (M)	Pakistani	12 wk	4.5	√	X	X	NR	Autistic spectrum disorder Hearing ↓	NPL	NPL	NAD
5	8 (F)	Pakistani	Birth	12	√	X	X	NR	Good	NPL	NPL	NAD
	9 (M)	British Caucasian	6 wk	21	√	X	Aversion	NR	Good	1.06	CF	Mild PSCLO
	10 (M)	British Caucasian	8 wk	19	√	√	Attraction	<5°	Good	0.42	0.66	Mild PSCLO

√, present; ?, unsure; X, absent; VF, visual fields; NR, nonrecordable; ND, not done; CF, count fingers; HM, hand movements; LP, light perception; NPL, nil light perception; PCIOL, posterior chamber intraocular lens implant; PSCLO, posterior subcapsular lens opacification; wk, weeks; NAD, nothing abnormal detected.

right eye and 1.48 logMAR in the left eye at age 17 years. Patient 10 had a BCVA of 0.22 logMAR in the right eye and 0.1 logMAR in the left eye at age 19 years, with correction of his refractive error (right eye +0.75 sphere/+3.25 cylinder at 87° and left eye +0.50 sphere/+3.50 cylinder at 85°). Goldmann perimetry in this patient revealed severe visual field constriction to less than 5° central field preservation (Fig. 1I). Slit lamp examination revealed keratoconus in patient 1 and mild cataract in patients 1, 9, and 10.

The fundi in all patients showed severe, widespread RPE atrophy and minimal intraretinal pigmentation, with relative parafoveal preservation (Figs. 1A, 1C, 1E). There was severe arteriolar attenuation and optic disc pallor. Bilateral optic disc drusen were present in patient 10. Severe nystagmus precluded the acquisition of fundus autofluorescence (FAF) imaging in most patients; however, in three subjects a parafoveal annulus of high-density AF was evident (Figs. 1B, 1D, 1F). Spectral domain OCT imaging was performed in patients 10 and 2 (Figs. 1G, 1H, respectively). High-quality OCT image acquisition was again limited due to nystagmus; however, the images obtained in both these patients demonstrated retinal thinning and a relatively preserved inner segment/outer segment junction at the fovea that, in patient 10, corresponded with the centrally preserved visual field on Goldmann perimetry (Fig. 1H, 1I). Elsewhere, there was loss of the photoreceptor layer.

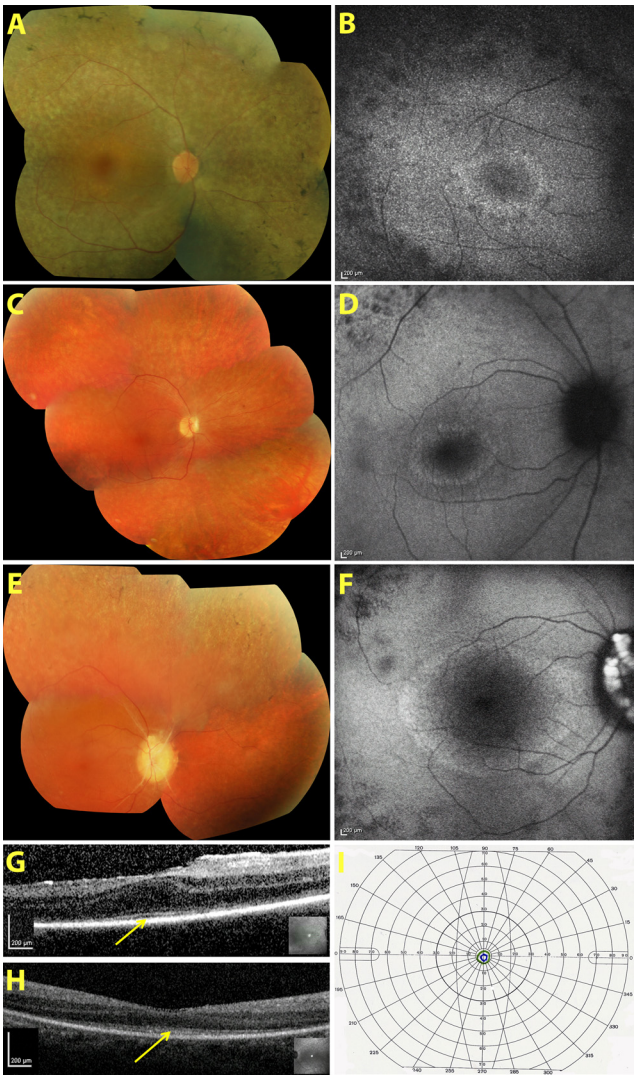

FIGURE 1. Clinical phenotype associated with *SPATA7* mutations. Fundus photographs of the right eye in subjects 5 (**A**), 9 (**C**), and 10 (**E**) show widespread retinal pigment epithelium atrophy with minimal peripheral intraretinal pigment migration, optic disc pallor, arteriolar attenuation, and parafoveal sparing. Patient 10 also had optic disc drusen. Fundus autofluorescence (AF) imaging demonstrated a parafoveal annulus of high-density AF (**B**, **D**, **F**). The optic disc drusen in patient 10 were more clearly visible on AF imaging (**F**). In patients 10 and 2, SD-OCT imaging demonstrated a relatively preserved foveal inner segment–outer segment junction (**G**, **H**, *arrows*), corresponding to the centrally preserved visual field seen on Goldmann perimetry to the I4e target (*blue* isopter) and V4e target (*green* isopter) in patient 10 (**I**).

Electroretinography in patient 3 was undertaken using corneal electrodes according to the recommendations of ISCEV, at age 18 years. PERGs were bilaterally undetectable, as were full-field rod and cone driven ERGs, in keeping with severe bilateral photoreceptor dysfunction. Electroretinography was performed in patients 9 and 10, by using skin and DTL electrodes and a modified pediatric ERG protocol. At 2 years of age, patient 10 had normal rod driven ERG b-wave amplitudes, but his photopic ERGs were not detectable. By 4 years of age, his rod driven b-wave amplitudes were subnormal, and by 9 years, they had become undetectable. His older brother (patient 9) was first tested at age 4 years when photopic ERGs were absent, but rod driven ERGs of subnormal amplitude were detected. One year later, at age 5 years, the rod ERG was also undetectable.

DISCUSSION

SPATA7 is a rare cause of LCA and severe childhood-onset retinal dystrophy with mutations identified in 1.7% of probands in this study. Eight mutations in *SPATA7* have been published to date. This report increases the number of known mutations to 11 and further delineates the phenotype associated with *SPATA7* mutations.

Three of the four mutations identified in this study would lead to premature termination of the protein. These occur early in the transcript (exons 5 and 8). It is predicted that these altered transcripts would be degenerated through nonsense mediated decay (NMD), a potential outcome in transcripts where an early stop codon is recognized. Only when the premature stop codon occurs in the last coding exon or the last 55 bp of the preceding exon are these transcripts protected from NMD.[31]

Since there is no known function for SPATA7 as yet, it is difficult to speculate on the effect of the loss of a histidine at position 409 on the protein (mutation identified in family 5). This deletion was not seen in any of the variation databases, nor was it found in the screening of 150 ethically matched controls (data not shown). In silico analysis of this mutation is difficult because little is known about the protein. Analysis using the GenTHREADER program[32] predicted no significant folding changes. Histidine at position 409 is conserved across species, such as humans, chimpanzee, dog, and chicken, but is either a glutamine or tyrosine in cow and rodents. All three amino acids are large, which may mean that loss of such a bulky amino acid would affect the folding of the protein, leaving it susceptible to removal from the cell.

Three families were found to be homozygous for p.R85X. Two are of Pakistani origin, with family 3 originally from Bangladesh. There is no evidence to suggest that these three families are related.

The identification of many SNPs in *SPATA7* has reiterated the problem of screening a candidate gene in a large number of patients. We initially wanted to use high-resolution melting curve analysis (Lightscanner; Idaho Technology) to screen the

whole gene in this cohort. The technique works well on amplimers that contain no SNPs and are less than 400 bp in length. We focused on using this technique on exons 2 to 5 but found that SNPs in exons 2, 4, and 5 complicated the analysis.

The ocular phenotype associated with *SPATA7* mutations is of a severe infantile-onset cone rod dystrophy. In this study, most individuals had a clinical diagnosis of LCA, but in one individual, there was a milder phenotype with near normal visual acuity. This patient had a mutation that may be associated with residual SPATA7 activity which may explain the milder phenotype. However, his older brother had severe disease, suggesting that other factors, such as the effects of modifier alleles, may be a more plausible explanation. Fundus examination in our patients showed severe RPE atrophy with little intraretinal pigment migration; the central macula had a relatively normal appearance. FAF imaging in three subjects, however, showed a parafoveal annulus of hyperautofluorescence, which has been reported in LCA and other retinal dystrophies.[33,34] High-definition SD-OCT imaging was possible in two subjects and in both showed retinal thinning and preservation of the inner segment–outer segment junction at the fovea. This study therefore shows *SPATA7* retinopathy to be an infantile-onset severe cone–rod dystrophy with early extensive peripheral retinal atrophy but with variable foveal involvement.

Previous papers reporting mutations in *SPATA7* have contained limited phenotypic information. Affected members of the original Saudi Arabian family described by Wang et al.,[15] with a homozygous p.R108X mutation, had poor visual fixation from birth, nystagmus, hypermetropic astigmatism, and an unrecordable ERG—features consistent with LCA.[15] There was no information about the fundus appearance or the results of retinal imaging. A Dutch patient with the same mutation was reported to have visual impairment and nystagmus from birth and, when examined at age 6 years, had peripheral chorioretinal atrophy and retinal pigmentation. Wang et al. also reported a 7-year-old girl, homozygous for p.R395X with juvenile-onset RP, who had 20/20 visual acuity, no nystagmus, early onset nyctalopia, 5° visual fields on Goldmann perimetry and undetectable ERG responses. The retina was gray with arteriolar narrowing and a diffuse hypopigmented parafoveal annulus. This patient had a phenotype similar to patient 10 in the present series, who also had one mutation affecting the final exon in *SPATA7*. In the series described by Wang et al., one patient with a homozygous frame shift mutation reported normal vision in childhood but subsequently developed nyctalopia and nystagmus. At 55 years of age he had advanced retinal pigmentary degeneration, narrow arterioles, optic disc pallor, and maculopathy. The ERG was undetectable, and visual fields were reduced to 5°.[15] Although no longitudinal clinical data are available for patients with *SPATA7* mutations, this case, and the younger subjects from the present series who showed deterioration in ERG responses with time, suggest that the retinal dystrophy is progressive.

Perrault et al.[22] described five patients with *SPATA7* mutations who also had clinical features consistent with LCA. They suggested that, since mutations would affect both isoforms of SPATA7, there may be an effect on male fertility, but they were unable to test this hypothesis, as their only male patient was 13 years old. In our cohort, patient 1 (family 1) had infertility, as did his affected brother. There were no fertility disorders in our other families (males in these families have not had problems conceiving children), suggesting that SPATA7 does not play a key role in male fertility.

SPATA7 mutations are a rare cause of LCA in the British population, accounting for 1.7% of disease. These patients presented in infancy with a severe retinal dystrophy similar to LCA. A small subset of patients may have a milder phenotype; however, even in these cases there is extensive visual field loss and deterioration of visual function with age. There is preservation of foveal architecture early in the course of the disease, and there may be a window of opportunity for therapy at this stage.

Acknowledgments

The authors thank the families for taking part in this study and Jill E. Urqhart and Sarah B. Daly at Manchester Academic Health Sciences Centre (MAHSC) for their technical assistant with the SNP array genotyping.

References

1. Leber T. Retinitis pigmentosa und angeborene amaurose. *Albert von Graefes Arch Ophthalmol*. 1869;15:1–25.
2. Heckenlively JR, Foxman SG, Parelhoff ES. Retinal dystrophy and macular coloboma. *Doc Ophthalmol.* 1988;68:257–271.
3. Foxman S, Heckenlively J, Bateman J, Wirtschafter J. Classification of congenital and early onset retinitis pigmentosa. *Arch Ophthalmol.* 1985;103:1502–1506.
4. Franceschetti A, Dieterle P. Diagnostic and prognostic importance of the electroretinalgram in tapetoretinal degeneration with reduction of the visual field and hemeralopia. *Confin Neurol.* 1954;14:184–186.
5. Perrault I, Rozet J-M, Calvas P, Gerber S, Camuzat A, Dollfus H. Retinal-specific guanylate cyclase gene mutations in Leber's congenital amaurosis. *Nat Genet.* 1996;14:461–464.
6. Sohocki MM, Bowne SJ, Sullivan LS, et al. Mutations in a new photoreceptor-pineal gene on 17p cause Leber congenital amaurosis. *Nat Genet.* 2000;24:79–83.
7. Marlhens F, Bareil C, Griffoin JM, Zrenner E, Amalric P, Eliaou C. Mutations in REP65 cause Leber's congenital amaurosis. *Nat Genet.* 1997;17:139–141.
8. Dryja T, Adams S, Grimsby J, et al. Null RPGRIP1 alleles in patients with Leber congenital amaurosis. *Am J Hum Genet.* 2001;68:1295–1298.
9. Freund CL, Wang Q-L, Chen S, et al. De novo mutations in the CRX homeobox gene associated with Leber congenital amaurosis. *Nat Genet.* 1998;18:311–312.
10. Hanein S, Perrault I, Gerber S, et al. Leber congenital amaurosis: comprehensive survey of the genetic heterogeneity, refinement of the clinical definition, and genotype-phenotype correlations as a strategy for molecular diagnosis. *Hum Mutat.* 2004;23:306–317.
11. den Hollander AI, Heckenlively JR, van den Born LI, et al. Leber congenital amaurosis and retinitis pigmentosa with Coats-like exudative vasculopathy are associated with mutations in the crumbs homologue 1 (CRB1) gene. *Am J Hum Genet.* 2001;69:198–203.
12. Janecke AR, Thompson DA, Utermann G, et al. Mutations in RDH12 encoding a photoreceptor cell retinol dehydrogenase cause childhood-onset severe retinal dystrophy. *Nat Genet.* 2004;36:850–854.
13. den Hollander AI, Koenekoop RK, Yzer S, et al. Mutations in the CEP290 (NPHP6) gene are a frequent cause of Leber congenital amaurosis. *Am J Hum Genet.* 2006;79:556–561.
14. den Hollander AI, Koenekoop RK, Mohamed MD, et al. Mutations in LCA5, encoding the ciliary protein lebercilin, cause Leber congenital amaurosis. *Nat Genet.* 2007;39:889–895.
15. Wang H, den Hollander AI, Moayedi Y, et al. Mutations in SPATA7 cause Leber congenital amaurosis and juvenile retinitis pigmentosa. *Am J Hum Genet.* 2009;84:380–387.
16. Thompson DA, Li Y, McHenry CL, et al. Mutations in the gene encoding lecithin retinol acyltransferase are associated with early-onset severe retinal dystrophy. *Nat Genet.* 2001;28:123–124.
17. Gal A, Li Y, Thompson DA, et al. Mutations in MERTK, the human orthologue of the RCS rat retinal dystrophy gene, cause retinitis pigmentosa. *Nat Genet.* 2000;26:270–271.
18. Estrada-Cuzcano A, Koenekoop RK, Coppieters F, et al. IQCB1 Mutations in patients with Leber congenital amaurosis. *Invest Ophthalmol Vis Sci.* 2011;52:834–839.

19. Keen TJ, Mohamed MD, McKibbin M, et al. Identification of a locus (LCA9) for Leber's congenital amaurosis on chromosome 1p36. *Eur J Hum Genet.* 2003;11:420–423.
20. Stockton DW, Lewis RA, Abboud EB, et al. A novel locus for Leber congenital amaurosis on chromosome 14q24. *Hum Genet.* 1998; 103:328–333.
21. Li Y, Wang H, Peng J, et al. Mutation survey of known LCA genes and loci in the Saudi Arabian population. *Invest Ophthalmol Vis Sci.* 2009;50:1336–1343.
22. Perrault I, Sylvain H, Xavier G, et al. Spectrum of SPATA7 mutations in Leber congenital amaurosis and delineation of the associated phenotype. *Hum Mutat.* 2010;31:E1241–E1250.
23. Zhang X, Liu H, Zhang Y, et al. A novel gene, RSD-3/HSD-31, encodes a meiotic-related protein expressed in rat and human testis. *J Mol Med.* 2003;81:380–387.
24. Mammalian Gene Collection (MGC) Program Team. Generation and initial analysis of more than 15,000 full-length human and mouse cDNA sequences. *Proc Natl Acad Sci U S A.* 2002;99: 16899–16903.
25. Marmor MF, Fulton AB, Holder GE, Miyake Y, Brigell M, Bach M. ISCEV Standard for full-field clinical electroretinography: 2008 update. *Doc Ophthalmol.* 2009;118:69–77.
26. Holder GE, Brigell MG, Hawlina M, et al. ISCEV standard for clinical pattern electroretinography: 2007 update. *Doc Ophthalmol.* 2007; 114:111–116.
27. Flitcroft DI, Adams GGW, Robson AG, Holder GE. Retinal dysfunction and refractive errors: an electrophysiological study of children. *Br J Ophthalmol.* 2005;89:484–488.
28. Kriss A. Skin ERGs: their effectiveness in paediatric visual assessment, confounding factors, and comparison with ERGs recorded using various types of corneal electrode. *Int J Psychophysiol.* 1994;16:137–146.
29. Carr IM, Flintoff KJ, Taylor GR, Markham AF, Bonthron DT. Interactive visual analysis of SNP data for rapid autozygosity mapping in consanguineous families. *Hum Mutat.* 2006;27:1041–1046.
30. Hubbard TJP, Aken BL, Beal K, et al. Ensembl 2007. *Nucleic Acids Res.* 2007;35:D610–D617.
31. Khajavi M, Inoue K, Lupski JR. Nonsense-mediated mRNA decay modulates clinical outcome of genetic disease. *Eur J Hum Genet.* 2006;14:1074–1081.
32. Lobley A, Sadowski MI, Jones DT. pGenTHREADER and pDomTHREADER: new methods for improved protein fold recognition and superfamily discrimination. *Bioinformatics.* 2009; 25:1761–1767.
33. Scholl HPN, Chong NHV, Robson AG, Holder GE, Moore AT, Bird AC. Fundus autofluorescence in patients with Leber congenital amaurosis. *Invest Ophthalmol Vis Sci.* 2004;45:2747–2752.
34. Robson A, Michaelides M, Saihan Z, et al. Functional characteristics of patients with retinal dystrophy that manifest abnormal parafoveal annuli of high density fundus autofluorescence; a review and update. *Doc Ophthalmol.* 2008;116:79–89.